

Sequestering Carbon Dioxide in Coalbeds

Technical Progress Report

Reporting Period
from September 28, 1998 to October 28, 1999

K. A. M. Gasem
R. L. Robinson, Jr.

Oklahoma State University
School of Chemical Engineering
Stillwater, Oklahoma 74078-0537

L. R. Radovic

Pennsylvania State University
Department of Energy and
Geo-Environmental Engineering
University Park, PA 16802

PREPARED FOR THE UNITED STATES
DEPARTMENT OF ENERGY
DE-FC26-98FT40426

DISCLAIMER

This report was prepared as an account of work sponsored by an agency of the United States Government. Neither the United States Government nor any agency thereof, nor any of their employees, makes any warranty, express or implied, or assumes any legal liability or responsibility for the accuracy, completeness, or usefulness of any information, apparatus, product, or process disclosed or represents that its use would not infringe privately owned rights. Reference herein to any specific commercial product, process, or service by trade name, trademark, manufacturer, or otherwise does not necessarily constitute or imply its endorsement, recommendation, or favoring by the United States Government or any agency thereof. The views and opinions of authors expressed herein do not necessarily state or reflect those of the United States Government or any agency thereof.

ABSTRACT

The authors' long term goal is to develop accurate prediction methods for describing the adsorption behavior of gas mixtures on solid adsorbents over complete ranges of temperature, pressure and adsorbent types. The major objectives of the project are to

- measure the adsorption behavior of pure CO₂, methane, nitrogen and their binary and ternary mixtures *on several selected coals having different properties* at temperatures and pressures applicable to the particular coal being studied,
- generalize the adsorption results in terms of appropriate properties of the coals, to facilitate estimation of adsorption behavior for coals other than those studied experimentally,
- delineate the sensitivity of the *competitive* adsorption of CO₂, methane and nitrogen to the specific characteristics of the coal on which they are adsorbed; establish the major differences (if any) in the nature of this competitive adsorption on different coals, and
- test and/or develop theoretically-based mathematical models to represent accurately the adsorption behavior of mixtures of the type for which measurements are made.

The specific accomplishments of this project during this reporting period are summarized below in three broad categories outlining experimentation, model development, and coal characterization.

Experimental Work: Our adsorption apparatus was reassembled, and all instruments were tested and calibrated. Having confirmed the viability of the experimental apparatus and procedures used, adsorption isotherms for pure methane, carbon dioxide and nitrogen on wet Fruitland coal were measured at 319.3 K (115 °F) and pressures to 12.4 MPa (1800 psia). These measurements showed good agreement with our previous data and yielded an expected uncertainty of about 2%. Preparations are underway to measure adsorption isotherms for pure methane, carbon dioxide and nitrogen on two other coals.

Model Development The experimental data were used to evaluate the predictive capabilities of various adsorption models, including the Langmuir/loading ratio correlation, two-dimensional cubic equations of state, and the local density model. In general, all models performed well for Type I adsorption exhibited by methane, nitrogen, and carbon dioxide up to 8.3 MPa (average deviations within 2%). However, for pressures higher than 8.3 MPa (1200 psia), carbon dioxide produced multilayer adsorption behavior similar to Type IV adsorption. Our results to date indicate that the SLD model may be a suitable choice for modeling multilayer coalbed gas adsorption. However, model improvements are required to (a) account for coal heterogeneity and structure complexity, and (b) provide for more accurate density predictions.

Coal Characterization: We have identified several well-characterized coals for use in our adsorption studies. The criteria for coal selection has been guided by the need for coals that (a) span the spectrum of properties encountered in coalbed methane production (such as variation in rank), and (b) originate from coalbed methane recovery sites (e.g., San Juan Basin, Black Warrior Basin, etc.).

At Pennsylvania State University, we have completed calibrating our instruments using a well-characterized activated carbon. In addition, we have conducted CO₂ and methane uptakes on four samples, including (a) a widely used commercial activated carbon, BPL from Calgon Carbon Corp. (reference material); (b) an Illinois #6 bituminous coal from the Argonne Premium Coal sample bank; (c) a Fruitland Intermediate coal sample; (d) a dry Fruitland sample. The results are as expected, except for a greater sensitivity to the outgassing temperature. "Standard" outgassing conditions (e.g., 383.2 K, overnight), which are often used, may not be appropriate for gas storage in coalbeds. Conditions that are more representative of in-situ coal (approximately 313.2 K) may be much more appropriate. In addition, our results highlight the importance of assessing the degree of approach to adsorption equilibrium.

TABLE OF CONTENTS

A. Executive Summary	6
B. Experimental Work	7
1. Experimental Facility	7
2. Experimental Methods and Procedures	7
C. Results and Discussion	9
1. Experimental Data	9
2. Model Development	9
D. Penn State Collaboration	15
D. Conclusions	17
E. References	18

A. Executive Summary

During the present reporting period, three complementary tasks involving experimentation, model development, and coal characterization were undertaken to meet our project objectives.

1. Our adsorption apparatus was reassembled, and all instruments were tested and calibrated. Having confirmed the viability of the experimental apparatus and procedures used, adsorption isotherms for pure methane, carbon dioxide and nitrogen on wet Fruitland coal were measured at 319.3 K (115 °F) and pressures to 12.4 MPa (1800 psia). These measurements showed good agreement with our previous data and yielded an expected uncertainty of about 2%. Preparations are underway to measure adsorption isotherms for pure methane, carbon dioxide and nitrogen on two other coals.
2. The experimental data were used to evaluate the predictive capabilities of various adsorption models, including the Langmuir/loading ratio correlation, two-dimensional cubic equations of state, and the local density model. In general, all models performed well for Type I adsorption exhibited by methane, nitrogen, and carbon dioxide up to 8.3 MPa (average deviations within 2%). However, for pressures higher than 8.3 MPa (1200 psia), carbon dioxide produced multilayer adsorption behavior similar to Type IV adsorption. Our results to date indicate that the SLD model may be a suitable choice for modeling multilayer coalbed gas adsorption. However, model improvements are required to (a) account for coal heterogeneity and structure complexity, and (b) provide for more accurate density predictions.
3. We have identified several well-characterized coals for use in our adsorption studies. The criteria for coal selection has been guided by the need for coals that (a) span the spectrum of properties encountered in coalbed methane production (such as variation in rank), and (b) originate from coalbed methane recovery sites (e.g., San Juan Basin, Black Warrior Basin, etc.).

At Pennsylvania State University, we have completed calibrating our instruments using a well-characterized activated carbon. In addition, we have conducted CO₂ and methane uptakes on four samples, including (a) a widely used commercial activated carbon, BPL from Calgon Carbon Corp. (reference material); (b) an Illinois #6 bituminous coal from the Argonne Premium Coal sample bank; (c) a Fruitland Intermediate coal sample; (d) a dry Fruitland sample. The results are as expected, except for a greater sensitivity to the outgassing temperature. "Standard" outgassing conditions (e.g., 383.2 K, overnight), which are often used, may not be appropriate for gas storage in coalbeds. Conditions that are more representative of in-situ coal (approximately 313.2 K) may be much more appropriate. In addition, our results highlight the importance of assessing the degree of approach to adsorption equilibrium.

B. Experimental Work

1. Experimental Facility

Experimental measurements to date have been made on apparatus developed in a prior project sponsored by Amoco Corporation and the Oklahoma Center for the Advancement of Science and Technology. As a precursor to the data acquisition, the apparatus was thoroughly re-tested and revised as necessary for operations in the present project. Details of the equipment design have been described previously [1,2]. A brief description of experimental methods and procedures is given in the following section.

In June 1999, we received a major equipment donation from BP Amoco. This should prove to be a major asset to the overall project. The donation consisted of essentially the complete coalbed methane research equipment housed at BP Amoco's Tulsa Technology Center. At the time of this report, this equipment is being reassembled in OSU's new Advanced Technology Research Center, a \$35 million state-of-the-art complex dedicated to research and technology development. Mr. Don Morgan, who formerly operated the equipment at BP Amoco, is now serving as a consultant in reassembling and validating this apparatus. We expect that it will be fully operational by August 1, 1999.

When operational, the new facility should allow us to essentially double our rate of data production. Although the efforts in reassembling, testing, and validating the new apparatus may cause minor temporary delays in data acquisition on the existing apparatus, the overall result should be to significantly increase the total amount of data produced by the end of the project.

In anticipation of the research equipment donation, we have purposely delayed purchase of certain equipment items identified in the initial proposal to the DOE. Now that the BP Amoco equipment is on hand, we are better positioned to acquire equipment that will be of maximum use to the project, without duplicating the equipment from BP Amoco. Specific items may include a gas chromatograph and/or a precision high-pressure injection pump.

2. Experimental Methods and Procedures

Our experimental technique employs a mass balance method, utilizing volumetric accounting principles. The experimental apparatus, shown schematically in Figure 1, has been used successfully in previous measurements [1, 2]. A brief description of the experimental apparatus and procedures follows.

The entire apparatus is maintained in a constant temperature air bath. The equilibrium cell (EC, Figure 1) is filled with the adsorbent to be studied, and the cell is placed under vacuum prior to gas injection. The void (gas) volume, V_{void} ,

in the equilibrium cell is then determined by injecting a known quantity of helium from a calibrated injection pump (P_2). Since helium is not adsorbed, the void volume can be determined from measured values of the temperature, pressure and amount of helium injected into the cell. The equations are

$$V_{\text{void}} = n_{\text{He}} (Z_{\text{He}} RT / p)_{\text{cell}} \quad (1)$$

$$n_{\text{He}} = (pV/Z_{\text{He}} RT)_{\text{pump}} \quad (2)$$

In these equations, n_{He} is the number of moles of helium injected into the cell, V is the volume of gas injected from the pump, Z_{He} is the compressibility factor of helium, R is the universal gas constant, T is the temperature, p is the pressure, and the subscripts "cell" and "pump" refer to conditions in the cell and pump sections of the apparatus, respectively.

The amount of gas (methane, for example) adsorbed at a given pressure can be calculated based on the preliminary calibrations done above. First, a given quantity of methane, n_{inj} , is injected into the cell. This amount is determined by an equation analogous to Equation 2, above. A recirculating pump is used to circulate methane over the adsorbent until equilibrium is reached, where no further methane is adsorbed. The amount of unadsorbed methane, n_{unads} , is then determined based on the fact that any unadsorbed methane will remain in the void volume determined from the helium calibration. The expression for this quantity is

$$n_{\text{unads}} = (pV_{\text{void}}/Z_{\text{methane}} RT)_{\text{cell}} \quad (3)$$

where the pressure p is measured after equilibrium is reached in the cell. The amount of adsorbed methane, n_{ads} , is then calculated by difference as

$$n_{\text{ads}} = n_{\text{inj}} - n_{\text{unads}} \quad (4)$$

These steps are repeated at sequentially higher pressures to yield a complete adsorption isotherm.

In mixture studies, the procedure is only slightly more complicated. The individual gases can be injected separately (or a gas mixture of known composition can be injected), so the total amount of each gas in the cell is known. The amount of unadsorbed gas at each pressure is calculated by Equation 3 with Z_{methane} replaced by Z_{mix} , the gas mixture compressibility factor. The composition of the gas mixture in the void volume is determined by chromatographic analysis of a microliter-size sample of the gas mixture captured in a sampling valve (SV_1). This permits the total amount of unadsorbed gas to be apportioned among the various components according to their mole fractions in the gas. Then, Equation 4 can be applied to each component in the gas mixture. For methane, nitrogen, and CO_2 mixtures, the mixture Z factor is determined accurately from available experimental data and accurate equations of state.

C. Results and Discussion

1. Experimental Data

Gas adsorption measurements for pure methane, nitrogen, and CO₂ on wet Fruitland coal at 115 °F are presented in Tables 1-3. Three replicate runs were conducted for each gas to confirm the precision of our measurements and to investigate the effect of variations in moisture content and coal sample preparation on the adsorption behavior. The present measurements cover the pressure range from 0.69 to 12.4 MPa (100 to 1800 psia).

The pure-gas adsorption behavior is illustrated in Figures 2-4, which indicate that the relative amounts of nitrogen, methane and CO₂ adsorbed are in the approximate ratio of 1/2/4. The figures also show that methane and nitrogen produce monolayer Type I adsorption. This is in contrast to the CO₂, which exhibits a multilayer adsorption at pressures exceeding 8.3 MPa (1200 psia), as shown in Figure 4. In all the figures, the smooth curves were generated from a Langmuir fit to our data.

Our error analysis indicates that the uncertainties for the pure-gas adsorption measurements are approximately 2%. These estimates, which are depicted as error bars in Figures 2-4, were generated by error propagation of uncertainties in all measured quantities. The estimated uncertainties in each of the experimentally measured quantities are as follows: temperature 0.2°F; pressure 0.2 psia; injected gas volume 0.02 cc. The newly acquired data confirm the estimated precision of our measurements and agree well with our previous data [2].

The present adsorption data were acquired using two coal samples of different moisture content. Both measurement sets indicate that water content values beyond the equilibrium water content do not significantly affect the adsorption behavior. This finding supports similar conclusion we have reached in previous studies [2, 3].

2. Model Development

We are currently investigating five avenues for representing adsorption equilibrium. These include (a) enhanced forms of the Langmuir-type isotherms (see, e.g., [4]), (b) two-dimensional equations of state, (c) the simplified local density models, (d) introduction of two-dimensional analogs of the activity coefficients used in vapor-liquid equilibrium calculations, and (e) treating adsorption as a constrained form of vapor-liquid equilibrium [5]. In so doing, our objective is to develop reliable, simple analytic models capable of describing multilayer adsorption of near-critical and supercritical components on heterogeneous surfaces.

In this report, we briefly outline the first three methods and discuss the quality of their representation of the methane, nitrogen and CO₂ pure-fluid adsorption.

(a) Langmuir Models

In general, simple models have been used to represent the behavior of pure and mixed gas adsorption on coal. The extended Langmuir model is used almost exclusively in literature studies [e.g., 5], although the Ideal Adsorbed Solution (IAS) model [6] has also been employed [7]. Both these models work well for essentially ideal adsorbed solutions, but neither is capable of handling nonidealities in the adsorbed phase with any accuracy. The extended Langmuir model is shown below as an illustration of the simple modeling approach used in most previous studies. For mixtures it takes the form

$$\theta = \frac{\omega_i}{L_i} = \frac{B_i p y_i}{1 + \sum_j B_j p y_j} \quad (5)$$

where ω_i is the amount of component "i" adsorbed (moles "i" adsorbed per unit mass of coal), L_i and B_i are Langmuir constants for "i", p is pressure, and y_i is the mole fraction of "i" in the gas phase. This relation allows mixture adsorption to be calculated from pure-component data, since values of L_i and B_i may be determined from the pure-component form of Equation 5.

The combined Langmuir-Freundlich adsorption isotherm, expressed in terms of ω_i , yields the loading ratio correlation (LCR) for mixtures

$$\theta = \frac{\omega_i}{L_i} = \frac{B_i (p y_i)^{\eta_i}}{1 + \sum_j B_j (p y_j)^{\eta_i}} \quad (6)$$

The additional parameter in the LRC (η_i) lends the Langmuir model more flexibility. Although the simplicity of Langmuir models is attractive, our data show that they are not adequate to represent the behavior of mixtures of the gases CO₂, methane, and nitrogen. In fact, previously we found errors greater than 100% when the extended Langmuir model was applied to our data on the adsorption of nitrogen from nitrogen + CO₂ mixtures [3].

(b) Equation-of-State Models

Simulations of coalbed gas recovery and CO₂ sequestering require reliable, yet simple analytic models beyond Langmuir-type correlations. Equation-of-state (EOS) frameworks offer an attractive potential for meeting such requirements.

If an adsorbed fluid is visualized as a two-dimensional nonideal compressed phase, it is appealing to use a two-dimensional analog of the van der Waals (VDW) EOS to describe pure adsorption isotherms and mixtures. Limited testing of the 2-D EOS approach has been reported, with generally unfavorable results [8, 9]. (Emphasis has been almost exclusively on the van der Waals form of the equation.) However, DeGance [10] demonstrated that, if properly applied, the 2-D EOS could perform well for adsorption on coal.

We have devised a generalized form of the 2-D EOS. The corresponding fugacity equations were derived to establish rigorous equilibrium relations between an adsorbed phase and a gas phase. The two-dimensional analog of any three-dimensional equation of state can be derived by proper selection of the parameters in the generalized equation. The van der Waals, Soave-Redlich-Kwong (SRK), Peng-Robinson (PR), Eyring, and a new 2-D EOS, have been applied to adsorption data on several systems, including highly nonideal systems.

A general form of the popular three-dimensional equations of state can be expressed by [11]:

$$\left[p + \frac{ap^2}{1 + Ub\omega + W(\omega)^2} \right] [1 - b\omega] = \rho RT \quad (7)$$

where a and b are the traditional EOS parameters, and numerical values of U and W may be specified to give various forms of three-dimensional equations of state. An even more general two-dimensional analog can be written as follows (by introducing an additional coefficient, m):

$$\left[A\pi + \frac{\alpha\omega^2}{1 + U\beta\omega + W(\beta\omega)^2} \right] [1 - (\beta\omega)^m] = \omega RT \quad (8)$$

where A is the specific surface area, π is the spreading pressure, ω is the specific amount adsorbed, and α and β are model parameters. The model coefficients, U , W , and m must be specified to obtain a specific form of the 2-D EOS for application. For example, an analog of the VDW EOS is obtained by setting $m = 1$ and $U = W = 0$, similarly for the SRK ($m = U = 1$ and $W = 0$), the PR ($m = 1$, $U = 2$, and $W = -1$), and the Eyring ($m = 1/2$ and $U = W = 0$) EOS.

This general 2-D EOS can be used to investigate EOS behaviors by specifying various combinations of model coefficients. Selection of the model coefficient m is the most important among the EOS model coefficients, because it has a significant effect on the shape of the pure adsorption isotherm. If U and W are equal to zero, then by setting m to values of ∞ , 1, and $1/2$, we obtain the 2-D ideal gas law, the VDW EOS, and the Eyring EOS, respectively. Actually, the pure gas isotherms

vary considerably in shape and we have found that it is sometimes desirable to select an m value even smaller than 1/2 to describe pure isotherms. Based on preliminary calculations, we have found that an equation with $m = 1/3$ and $U = W = 0$ (ZGR EOS) is promising [12]. The 2-D EOS can be applied to adsorbed phases containing mixtures by utilizing the traditional mixing rules (where x is the mole fraction in the adsorbed phase):

$$\alpha = \sum_i \sum_j x_i x_j \alpha_{ij} \quad (9)$$

$$\beta = \sum_i \sum_j x_i x_j \beta_{ij} \quad (10)$$

where

$$\begin{aligned} \alpha_{ij} &= (1 - C_{ij})(\alpha_i + \alpha_j)/2 \\ \beta_{ij} &= \sqrt{\beta_i \beta_j} \end{aligned} \quad (11)$$

Our experience to date indicates that the 2-D EOS approach is, in general, superior to the more widely-used theories such as the Ideal Adsorbed Solution (IAS) and extended Langmuir isotherm. However, this approach is inherently deficient in representing multilayer adsorption; especially, when it is applied to heterogeneous surfaces as in the case of coal.

Therefore, we are currently attempting to augment the EOS framework and render it useful for multilayer adsorption by (a) using solid-fluid site characterization based on characteristic curves similar to those generated by the Polanyi potential theory (see, e. g., [13]), and (b) superimposing the fluid-solid potential on an improved EOS phase description to predict the near-critical adsorption behavior. The latter is well exemplified by the simplified local density (SLD) model (see, e.g., Lira and coworkers [14]). We believe such developments will facilitate the use of highly efficient EOS computational frameworks for representing adsorption behavior, as well as improve our understanding of the phenomenon.

(c) The Simplified Local Density Model

The SLD model is a compromise between the traditional empirical and semi-empirical methods, which are computationally less demanding but are unable to account for the various adsorption isotherms seen near the critical region, and the computationally intensive molecular simulation methods. In applying the SLD adsorption model, the fluid-solid potential is superimposed on an equation of state (EOS) and the configurational energy integral in the inhomogeneous fluid phase is simplified with a local density approximation [14].

In this study, we evaluate the predictive capability of the SLD model for the supercritical adsorption systems encountered in CO_2 sequestering and coalbed methane recovery. Specifically, we correlate the experimental data on the adsorption of methane, nitrogen and carbon dioxide on wet Fruitland coal. The

SLD model predictions are then compared to the predictions obtained from the Langmuir, LRC, and the 2-D EOS models.

The SLD model is formulated in terms of the surface excess adsorption (Γ^{ex}), defined as the excess number of moles per unit area of adsorbent, or

$$\Gamma^{ex} = \int_{Z_0}^{\infty} (\rho(z) - \rho_{bulk}) dz \quad (12)$$

The lower limit of integration is the surface of the solid and is taken as the plane at $z_0 = \sigma_{ff}/2$, where σ_{ff} is the molecular distance between two solid molecules.

In adsorption, the SLD model asserts that the equilibrium chemical potential at any point z above the adsorbent surface is equal to the bulk phase chemical potential. Accordingly, the equilibrium chemical potential is calculated by contributions from fluid-fluid and fluid-solid interaction as

$$\mu = \mu_{bulk} = \mu_{ff}(z) + \mu_{fs}(z) \quad (13)$$

where the subscript bulk refers to the bulk fluid, ff refers to fluid-fluid interactions, fs refers to the fluid-solid interactions.

The fluid-solid potential at a given point z is independent of temperature and the number of molecules at and around that point. The fluid-solid potential is given in terms of the molecular interactions potential $\psi(z)$ and N_A is Avogadro's Number as

$$\mu_{fs} = N_A \Psi(z) \quad (14)$$

Lee's partially integrated 10-4 Lennard-Jones potential [8] is used to describe the adsorbate -adsorbent interactions

$$\Psi(z) = 4\pi \rho_{atom} \varepsilon_{fs} \sigma_{fs}^6 \left(\frac{\sigma_{fs}^6}{5x_1^{10}} - \frac{1}{2} \sum_{i=1}^4 \frac{1}{x_i^4} \right) \quad (15)$$

where ε_{fs} is the fluid-solid interaction energy parameter, $\rho_{atoms} = 0.382 \text{ \AA}^{-3}$, x is the intermolecular distance between fluid-molecule centers and the i th plane of solid molecules, σ_{fs} is taken as the arithmetic mean of the fluid and solid diameters. As indicated by Equation 15, the interactions are truncated at the fourth plane of solid atoms with an interplanar spacing of 3.35 \AA^0 .

The fluid-fluid potential is then calculated as

$$\mu_{ff} = \mu_{bulk} - N_A \Psi(z) \quad (16)$$

where

$$\begin{aligned}\mu_{\text{bulk}} &= \mu_{\circ} + RT \ln(f_{\text{bulk}} / f_{\circ}) \\ \mu_{\text{ff}} &= \mu_{\circ} + RT \ln(f_{\text{ff}}(z) / f_{\circ})\end{aligned}$$

After rearrangement this leads to

$$f_{\text{ff}}(z) = f_{\text{bulk}} \exp[-\Psi(z)/(kT)] \quad (17)$$

In this study, we have used the PR and PGR equations of state to determine the fluid and the bulk fugacities. The fugacity expressions for the PR EOS are (similar expressions for the PGR EOS are given elsewhere [15])

$$\begin{aligned}f_{\text{bulk}} &= RT / (v - b) \exp[b / (v - b) - 2a_{\text{bulk}} / (vRT)] \\ f_{\text{ff}} &= RT / [v(z) - b] \exp\{b / [v(z) - b] - 2a(z) / [v(z)RT]\}\end{aligned} \quad (18)$$

where a_{bulk} is the PR EOS constant, and $a(z)$ is evaluated as follows

$$a(z) = a_{\text{bulk}} \left(\frac{5}{16} + \frac{6}{16} \frac{z}{\sigma_{\text{ff}}} \right) \quad \text{for } 0.5 \leq \frac{z}{\sigma_{\text{ff}}} \leq 1.5 \quad (19)$$

$$a(z) = a_{\text{bulk}} \left[1 - \frac{1}{8 \left(\frac{z}{\sigma_{\text{ff}}} - \frac{1}{2} \right)^3} \right] \quad \text{for } 1.5 \leq \frac{z}{\sigma_{\text{ff}}} < \infty \quad (20)$$

Once the fugacity at the local point is determined, the EOS is used to calculate the corresponding local density $\rho(z)$. To apply the PR-SLD model, we have assumed that (a) the pure fluids are adsorbed on flat, homogenous coal surface, and (b) the coal has pseudo-crystalline structure. Details of our calculation procedure are given elsewhere [15].

(d) Model Evaluation Results

Tables 4-5 present a summary of our model evaluation results for the five models we used to correlate the present adsorption data for methane, nitrogen, and CO₂. The models include the Langmuir and LCR correlations, the ZGR and PGR 2-D EOS, and the PR-SLD model. The model parameters, shown in Table 5, were determined by minimizing the sum of squares of percentage absolute errors in the calculated adsorption, ω , for the pure gas of interest. The quality of the fit, expressed in terms of the absolute average deviation (%AAD), is given in Table 4. Figures 5-6 illustrate the abilities of the LRC, the ZGR EOS, and SLD model to describe the present pure-fluid adsorption data.

Our results indicate that the LRC produces better quality fit than the Langmuir correlation for the three gases studied (within 2% AAD), reflecting in part the use of one additional parameter (η_j) in the regressions. The results also reveal the ability of the ZGR EOS to represent the present systems well within their expected experimental uncertainty (within 2% AAD). By comparison, the PR-SLD model exhibits good representation for methane adsorption comparable to the LRC, but it exhibits larger deviations for the nitrogen and CO_2 (2.9% and 5.9%, respectively). The PR-SLD model results are not surprising in light of the assumptions made regarding the structure of the coal surface and the accuracy of the density predictions from of the PR EOS.

In these regressions, the data for CO_2 were restricted to pressures below 1000 psia, since all models, other than the SLD model, are inherently incapable of representing multilayer adsorption, which occurs at higher pressures for CO_2 .

Our results to date indicate that the SLD model may be a suitable choice for modeling the coalbed gas adsorption and CO_2 sequestering. However, model improvements are required to (a) account for coal heterogeneity and structure complexity, and (b) provide for more accurate equations of state, which are capable of modeling coalbed gas environments. In addition, future work will also address the competitive adsorption of mixed gases on coal.

D. Penn State Collaboration

During this year, two pieces of equipment were being refurbished for this project: a differential microcalorimeter and a low-pressure volumetric adsorption apparatus capable of operating with N_2 at 77 K and with CO_2 at 273 K. The calorimeter became operational first and, therefore, all experiments described in this report were performed with it.

Four samples were analyzed: (a) a widely used commercial activated carbon, BPL from Calgon Carbon Corp., which served as a convenient reference material; (b) an Illinois #6 bituminous coal from the Argonne Premium Coal sample bank; (c) a Fruitland Intermediate coal sample, from a well preserved core obtained in a previous coalbed methane project; (d) a dry Fruitland sample, obtained from the Oklahoma State University.

Figures 6 and 7 summarize the calibration results obtained with the BPL activated carbon. As expected, the uptakes and the adsorption heats were higher for CO_2 than for CH_4 . This is, of course, necessary for effective CO_2 sequestration in coalbeds. The heats are also in good agreement with the API data (Table 15A1.12), which give values of ca. 16 kJ/mol for CH_4 and ca. 29 kJ/mol for CO_2 . The results are moderately sensitive to the conditions of sample preparation: an increase in the outgassing temperature, from 80 to 150 °C, caused a small though inconsistent change in the uptake and very little change in the adsorption heats.

Figures 8 and 9 summarize the results obtained with the Illinois #6 coal. As expected, the uptakes are lower than those on the high-surface-area activated carbon, but the trends are the same: higher uptakes and higher adsorption heats for CO₂ than for CH₄. The effect of the outgassing temperature is important both from a fundamental and a practical point of view: most experimental data available in the literature, which were not obtained with CO₂ sequestration in mind, may have been obtained after inappropriate "sample preparation." For our purposes, an *in situ* temperature of ca. 40 °C seems the most appropriate. In our future studies, we shall use this outgassing temperature consistently, but we shall also attempt to understand the effects of changes in outgassing conditions.

Similar results are obtained with the Fruitland coal samples. (The Fruitland seam has been a site of intense coalbed methane research and development over the last decade.) Comparable trends are observed for the two samples, even though both the uptakes and the adsorption heats are larger for the "dry Fruitland" sample. One possible reason for these differences, apart from any differences in chemical composition or experimental error, is that the "dry Fruitland" sample consists of much smaller particles than the "Fruitland Intermediate" sample (which was obtained from chips during the coring process). These results highlight the importance of assessing the degree of approach to adsorption equilibrium: coals are known to be molecular-sieving adsorbents, even for small molecules such as CO₂ and CH₄, and the dynamics of CH₄ displacement by CO₂ will therefore be of interest in future studies.

E. Conclusions

Following is a summary of our accomplishments and conclusions:

- Our adsorption apparatus was reassembled, and all instruments were tested and calibrated.
- We have measured the adsorption behavior of pure CO₂, methane, ethane, nitrogen and some of their binary mixtures on wet Fruitland coal at temperatures at 319.3 K (115 °F) and pressures to 12.4 MPa (1800 psia). These measurements showed good agreement with our previous data and yielded an expected uncertainty of about 2%. Preparations are underway to measure adsorption isotherms for pure methane, carbon dioxide and nitrogen on two other coals. The newly-acquired data constitute a valuable addition to existing coalbed adsorption database.
- We have evaluated the predictive capabilities of various of various adsorption models, including the Langmuir/loading ratio correlation, two-dimensional cubic equations of state, and the local density model. In general, all models performed well for Type I adsorption exhibited by methane, nitrogen, and carbon dioxide up to 8.3 MPa (average deviations within 2%). However, for pressures higher than 8.3 MPa (1200 psia), carbon dioxide produced multilayer adsorption behavior similar to Type IV adsorption. Our results to date indicate that the SLD model may be a suitable choice for modeling multilayer coalbed gas adsorption. However, model improvements are required to (a) account for coal heterogeneity and structure complexity, and (b) provide for more accurate density predictions.
- We have identified several well-characterized coals for use in our adsorption studies. The criteria for coal selection has been guided by the need for coals that (a) span the spectrum of properties encountered in coalbed methane production, and (b) originate from coalbed methane recovery sites.
- At Pennsylvania State University, we have completed calibrating our instruments using a well-characterized activated carbon. In addition, we have conducted CO₂ and methane uptakes on four samples, including (a) a widely used commercial activated carbon, BPL from Calgon Carbon Corp. (reference material); (b) an Illinois 6 bituminous coal from the Argonne Premium Coal sample bank; (c) a Fruitland Intermediate coal sample; (d) a dry Fruitland sample. The results are as expected, except for a greater sensitivity to the outgassing temperature. "Standard" outgassing conditions (e.g., 383.2 K, overnight), which are often used, may not be appropriate for gas storage in coalbeds. Conditions that are more representative of in-situ coal (approximately 313.2 K) may be much more appropriate. In addition, our results highlight the importance of assessing the degree of approach to adsorption equilibrium.

F. References

1. Seidle, J. P., Jeansson, M. W., and Erickson, D. J., *Application of Matchstick Geometry to Stress Dependent Permeability in Coals*, SPE Paper 24361, presented at the Rocky Mountains Regional Meeting, Casper, WY, May 18-21, 1992.
2. Hall, F. E., Zhou, Chunhe, Gasem, K. A. M., and Robinson, Jr., R. L., *Adsorption of Pure Methane, Nitrogen, and Carbon Dioxide and their Binary Mixtures on Wet Fruitland Coal*, SPE Paper 29194, presented at the 1994 Eastern Regional Conference & Exhibition, Charleston, West Virginia, November 8-10, 1994.
3. Hall, F. E., *Adsorption of Pure and Multicomponent Gases on Wet Fruitland Coal*, M. S. Thesis, Oklahoma State University, December 1993.
4. Kapoor, A., Ritter, J. A., and Yang, R. T., *An Extended Langmuir Model for Adsorption of Gas Mixtures on Heterogeneous Surfaces*, Langmuir 6 660-664 (1990).
5. Arri, L. E., and Yee, D., *Modeling Coalbed Methane Production With Binary Gas Sorption*, SPE Paper 24363, presented at the SPE Rocky Mountain Regional Meeting, Casper, Wyoming, May 18-21, 1992.
6. Myers, A. L., and Prausnitz, J. M., *Thermodynamics of Mixed-Gas Adsorption*, AIChE J. 11 121-129 (1965).
7. Stevenson, M. D., Pinczewski, W. V., Somers, M. L., and Bagio, S. E., *Adsorption/Desorption of Multicomponent Gas Mixtures on Coal at In-Seam Conditions*, SPE Paper 23026, presented at the SPE Asia-Pacific Conference, Perth, Western Australia, November 4-7, 1991.
8. Danner, R. P., and Choi, E. C. F., *Mixture Adsorption Equilibria of Ethane and Ethylene on 13X Molecular Sieves*, Ind. Eng. Chem. Fundam. 17 248-253 (1978).
9. Suwanayuen, S., and Danner, R. P., *Vacancy Solution Theory of Adsorption From Gas Mixtures*, AIChE J 26 76-83 (1980).
10. DeGance, A. E., *Multicomponent High-Pressure Adsorption Equilibria on Carbon Substrates: Theory and Data*, Fluid Phase Equilibria, 78 99-137 (1992).
11. Chaback, J. J., Yee, D., Volz, R. R., Seidle, J. P., and Puri, R., *Method for Treating a Mixture of Gaseous Fluids within a Solid Carbonaceous Subterranean Formation*, U. S. Patent 5,439,054.

12. Zhou, C., Gasem, K. A. M., and Robinson, Jr., R. L., *Predicting Gas Adsorption Using Two -Dimensional Equations of State*, I&EC Research 33 1280-1289 (1994).
13. Ross, S., and Oliver, J. P., On Physical Adsorption, Interscience Publ., New York, 1964.
14. Rangarajan, B., Lira, T. C., and Subramanian, *Simplified Local Model for Adsorption over Large Pressure Ranges*, AIChE J., 41 838-845 (1995).
15. Liang, E., *Adsorption of Pure and Multicomponent Gases on Wet Fruitland Coal*, M. S. Thesis, Oklahoma State University, July 1999.

Table 1. Pure Methane Absolute Adsorption on Wet Fruitland Coal at 115 °F

RUN 1 (9.7%)*		RUN 2 (8.3%)		RUN 3 (7.6%)	
Pressure psia	Absolute Adsorption mmol/gcoal	Pressure psia	Absolute Adsorption mmol/gcoal	Pressure psia	Absolute Adsorption mmol/gcoal
112.1	0.2378	102.6	0.1942	106.9	0.2018
208.1	0.3427	208.1	0.3169	209.1	0.3213
395.1	0.4782	398.9	0.4650	403.7	0.4645
607.2	0.5860	608.0	0.5771	602.0	0.5674
805.0	0.6607	808.0	0.6547	804.1	0.6462
1008.2	0.7224	1004.8	0.7160	1006.4	0.7085
1214.8	0.7487	1207.0	0.7538	1207.9	0.7504
1404.9	0.7950	1407.3	0.7931	1405.9	0.7971
1602.8	0.8398	1605.7	0.8325	1601.8	0.8317
1801.8	0.8847	1802.3	0.8676	1800.4	0.8710

* Water content in the coal sample

Table 2. Pure Nitrogen Adsorption on Wet Fruitland Coal at 115 °F

RUN 1 (10.2%)		RUN 2 (9.9%)		RUN 3 (6.2%)	
Pressure psia	Absolute Adsorption mmol/gcoal	Pressure psia	Absolute Adsorption mmol/gcoal	Pressure psia	Absolute Adsorption mmol/gcoal
107.8	0.0489	105.6	0.0522	102.6	0.0470
210.6	0.0939	206.7	0.0902	201.9	0.0850
403.7	0.1487	402.5	0.1511	399.5	0.1495
602.5	0.2000	616.5	0.2050	603.3	0.2043
805.9	0.2498	804.9	0.2447	802.8	0.2511
1007.9	0.2812	1008.5	0.2848	1002.4	0.2912
1207.9	0.3155	1204.4	0.3167	1203.0	0.3215
1405.9	0.3419	1406.7	0.3527	1402.5	0.3516
1607.6	0.3640	1607.8	0.3817	1601.1	0.3800
1805.0	0.3934	1801.8	0.4041	1799.9	0.4002

Table 3. Pure Carbon Dioxide Adsorption on Wet Fruitland Coal at 115 °F

RUN 1 (9.0%)		RUN 2 (6.3%)		RUN 3 (5.1%)	
Pressure psia	Absolute Adsorption mmol/gcoal	Pressure psia	Absolute Adsorption mmol/gcoal	Pressure psia	Absolute Adsorption mmol/gcoal
105.1	0.508	105.2	0.502	102.1	0.462
210.0	0.695	200.5	0.667	210.7	0.692
402.1	0.919	399.2	0.907	407.5	0.920
612.4	1.037	602.9	1.039	601.2	1.026
798.0	1.115	803.5	1.134	802.3	1.138
1006.7	1.181	1007.0	1.218	1000.1	1.229
1205.5	1.312	1201.6	1.423	1203.1	1.380
1387.4	2.327	1383.5	2.514	1396.3	2.726
1490.2	3.915	1547.8	5.224	1559.6	5.588
1791.8	6.450	1772.3	6.778	1781.8	6.839

Table 4. Summary of the Model Results for Gas Adsorption on Wet Fruitland Coal at 115 °F

Model	No. of Parameters	% Deviation		
		Methane (30)*	Nitrogen (30)	Carbon Dioxide (18)
Langmuir	2	2.9	2.1	2.3
LRC	2	2.0	1.7	1.6
ZGR EOS	3	1.6	1.6	1.3
PR-SLD	2	1.9	2.9	5.1

* Number of data points

Table 5. Regression Results for Adsorption of Methane, Nitrogen, and Carbon Dioxide on Wet Fruitland Coal at 115 °F

Models	Model Parameters	Pure Gas Adsorbed		
		Methane (0-1800 psia)	Nitrogen (0-1800 psia)	Carbon Dioxide (0-1000 psia)
Langmuir	B_i	0.001953	0.000626	0.004487
	L_i	1.099	0.7428	1.445
LCR	η_i	0.87	0.87	0.87
	B_i	0.003448	0.000954	0.007518
	L_i	1.234	1.011	1.580
ZGR EOS	$\alpha_i \times 10^{-4}$	5.080	-2.261	0.8265
	β_i	0.4298	0.001	0.1661
	$-\ln k_i$	1.779	4.736	0.4587
PR-SLD	ε_{ff}	44.9	24.04	49.16
	SA	125.90	128.40	92.01

Figure 1. Schematic Diagram of Adsorption Apparatus

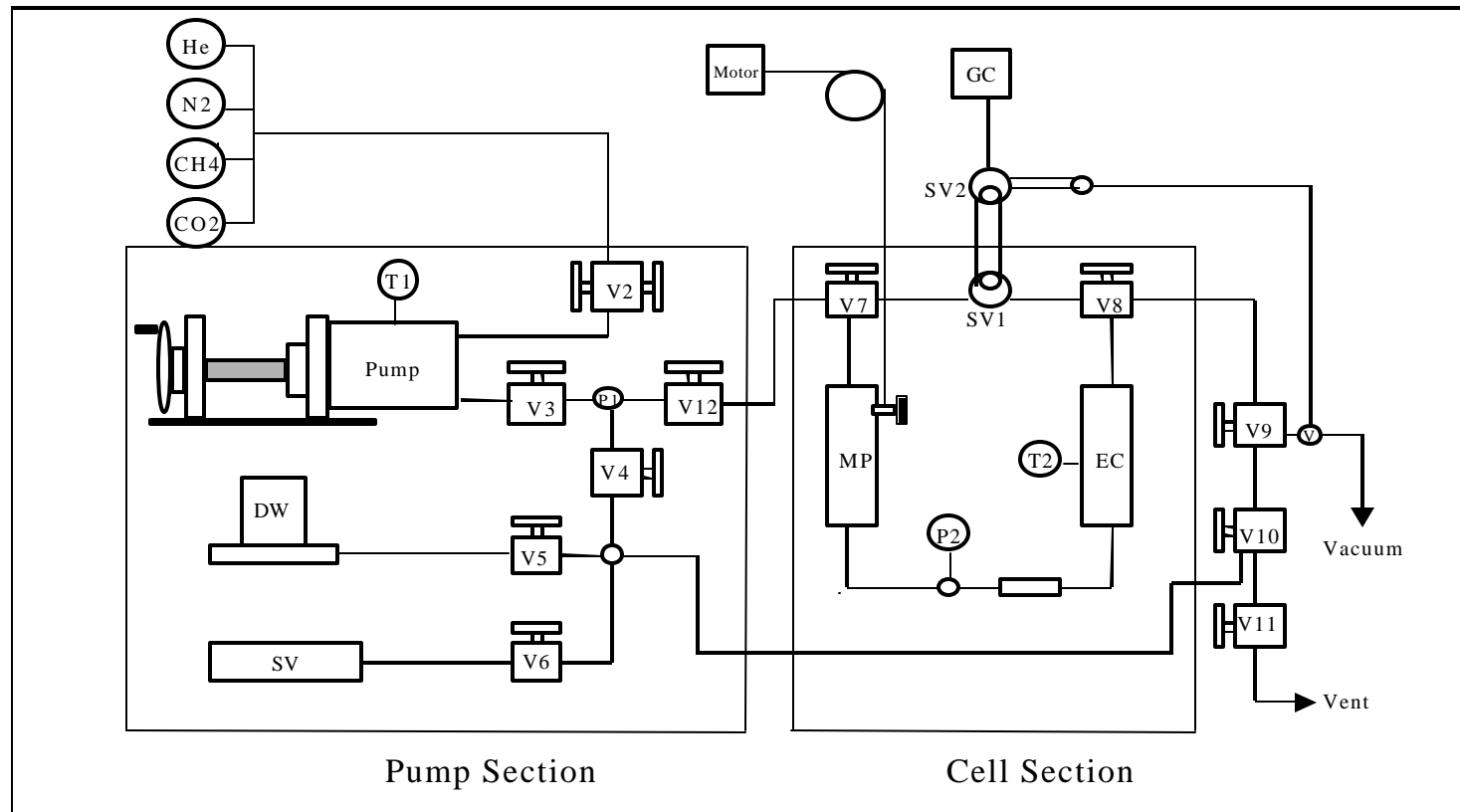


Figure 2. Pure Methane Adsorption on Wet Fruitland Coal at 115°F

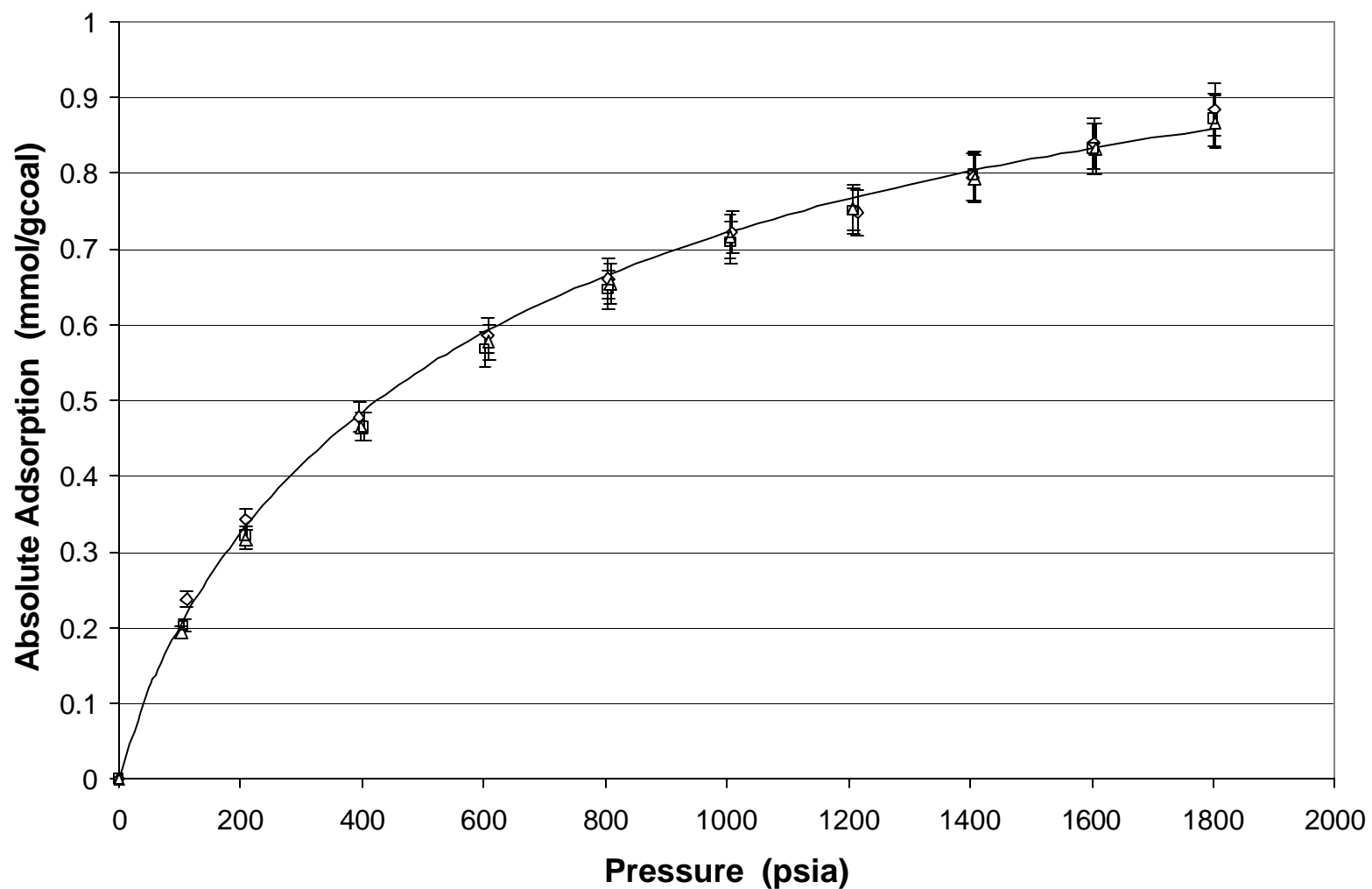
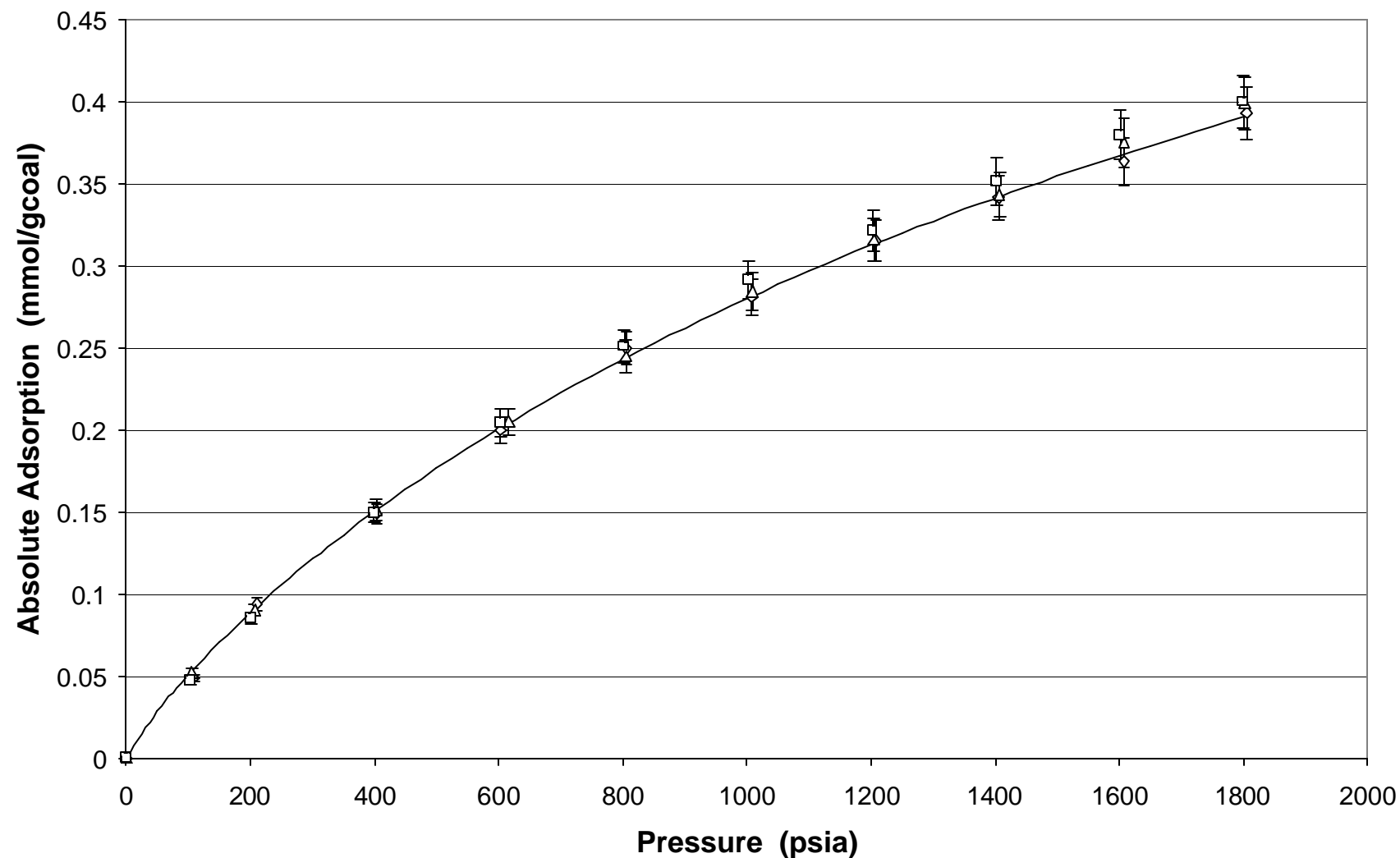


Figure 3. Pure Nitrogen Adsorption on Wet Fruitland Coal at 115°F



**Figure 4. Pure Carbon Dioxide Adsorption on Wet Fruitland Coal
at 115°F**

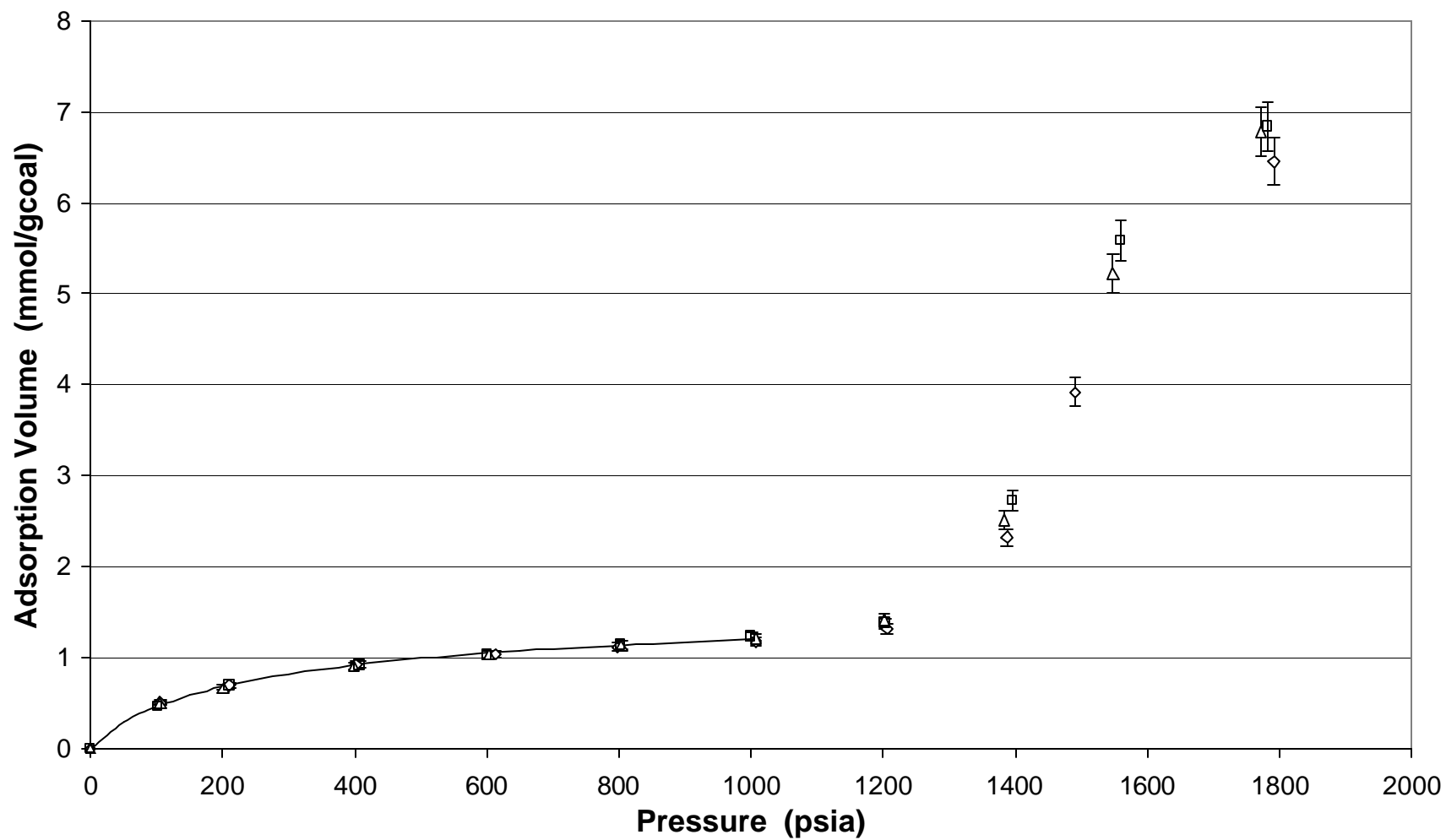


Figure 5. Prediction of Pure Gas Adsorption on Wet Fruitland Coal at 115°F Using LCR, ZGR EOS and PR-SLD Models

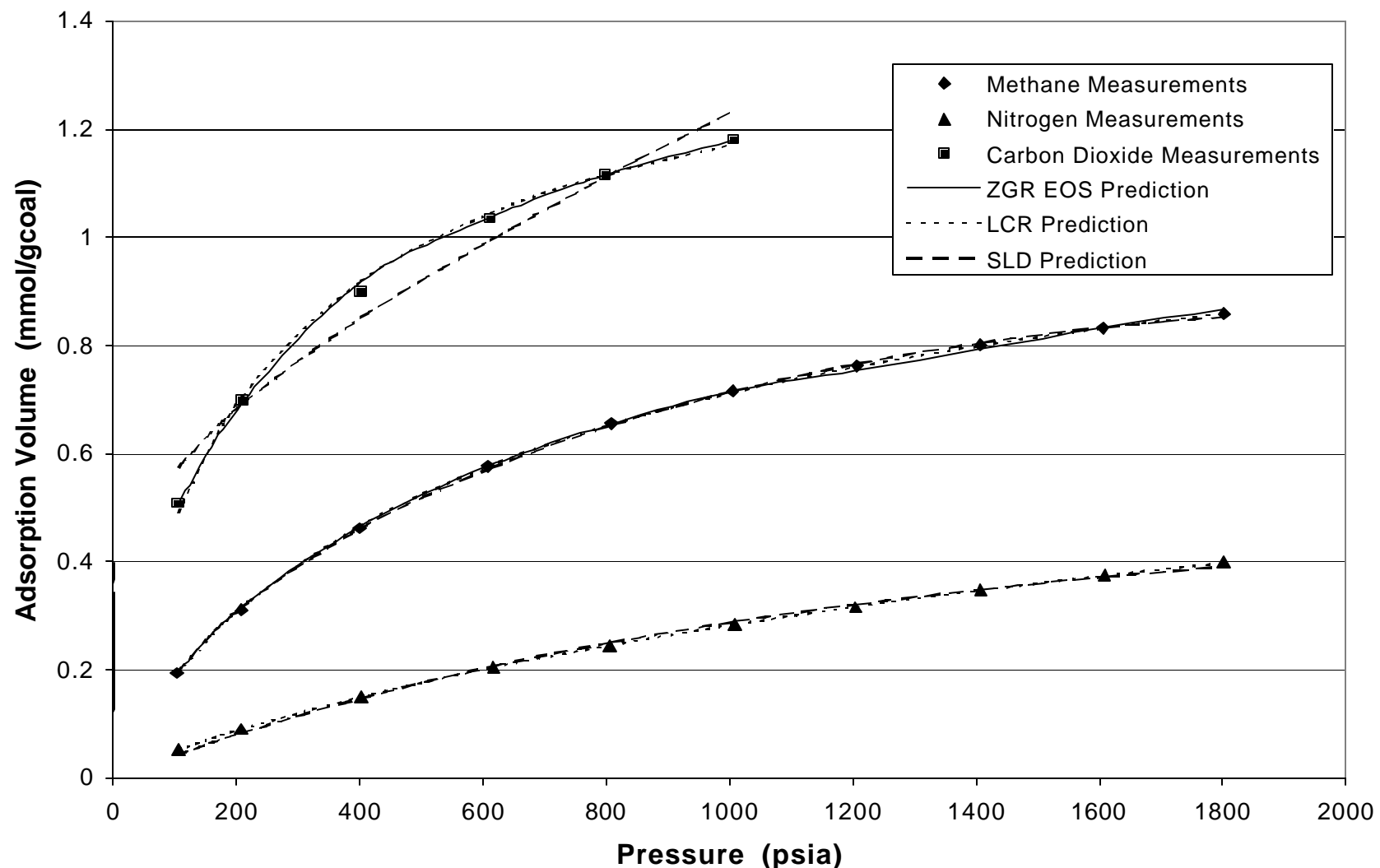


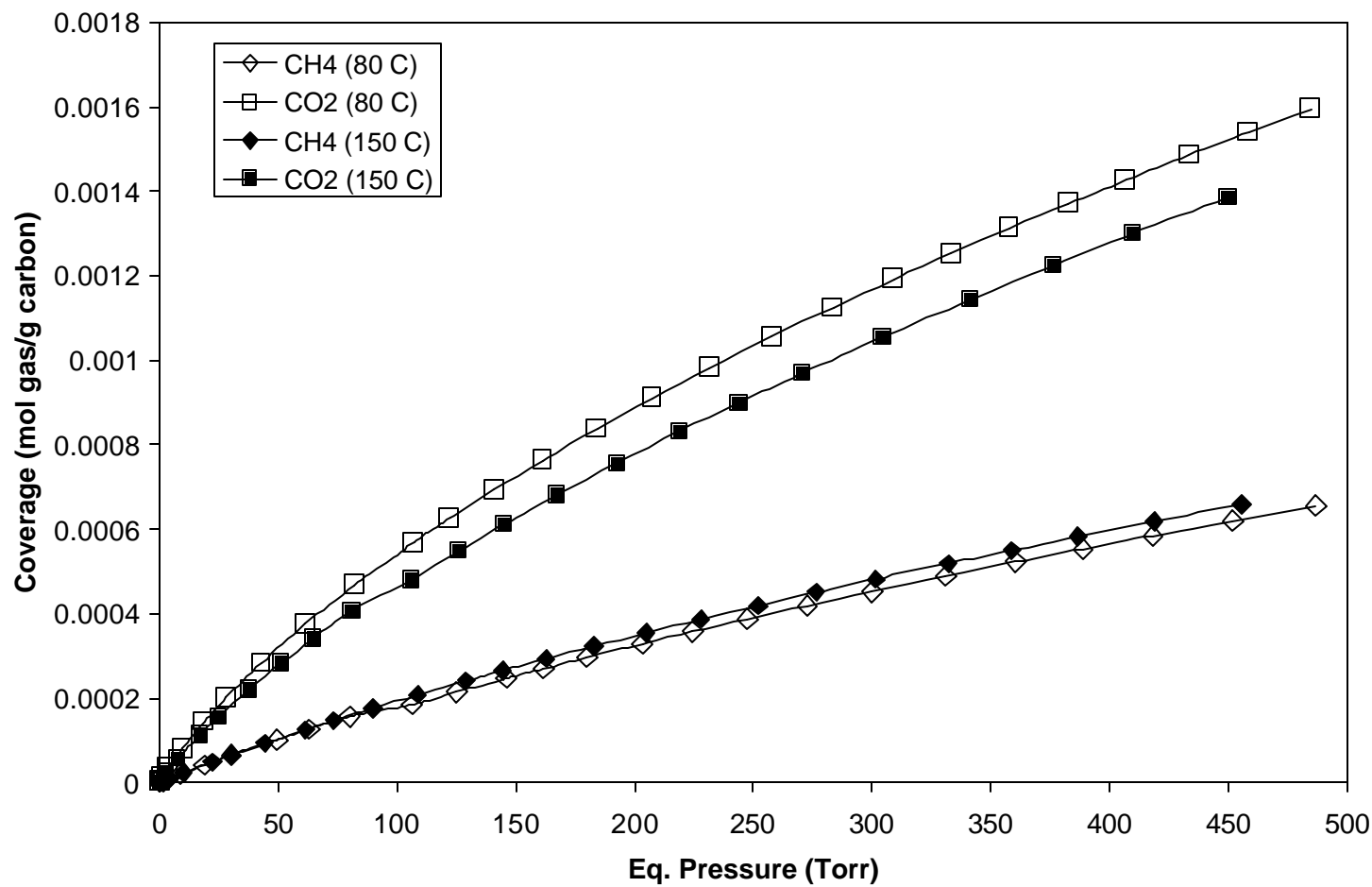
Figure 6. Gas Adsorption on BPL Carbon

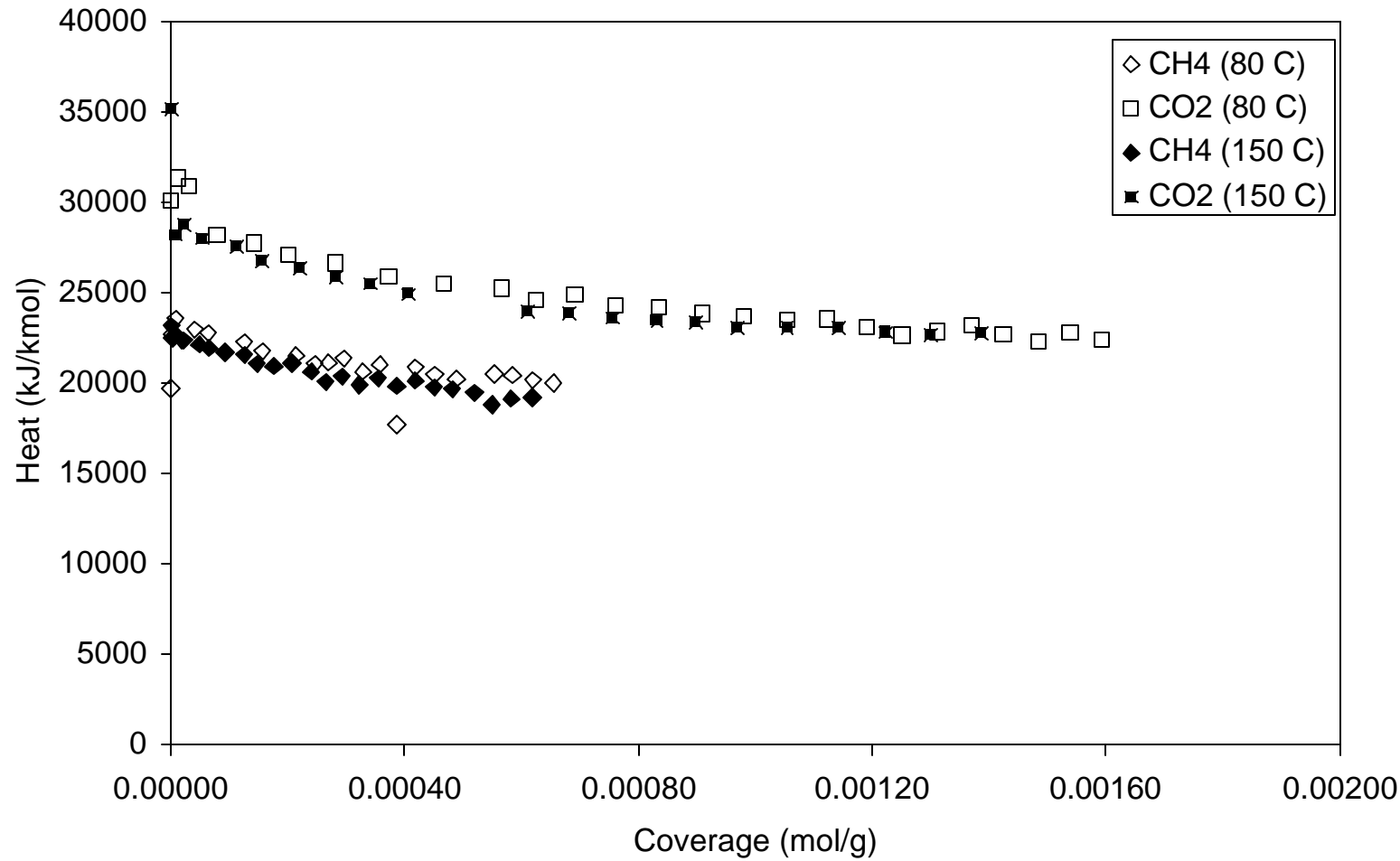
Figure 7. Heats of Adsorption on BPL Carbon

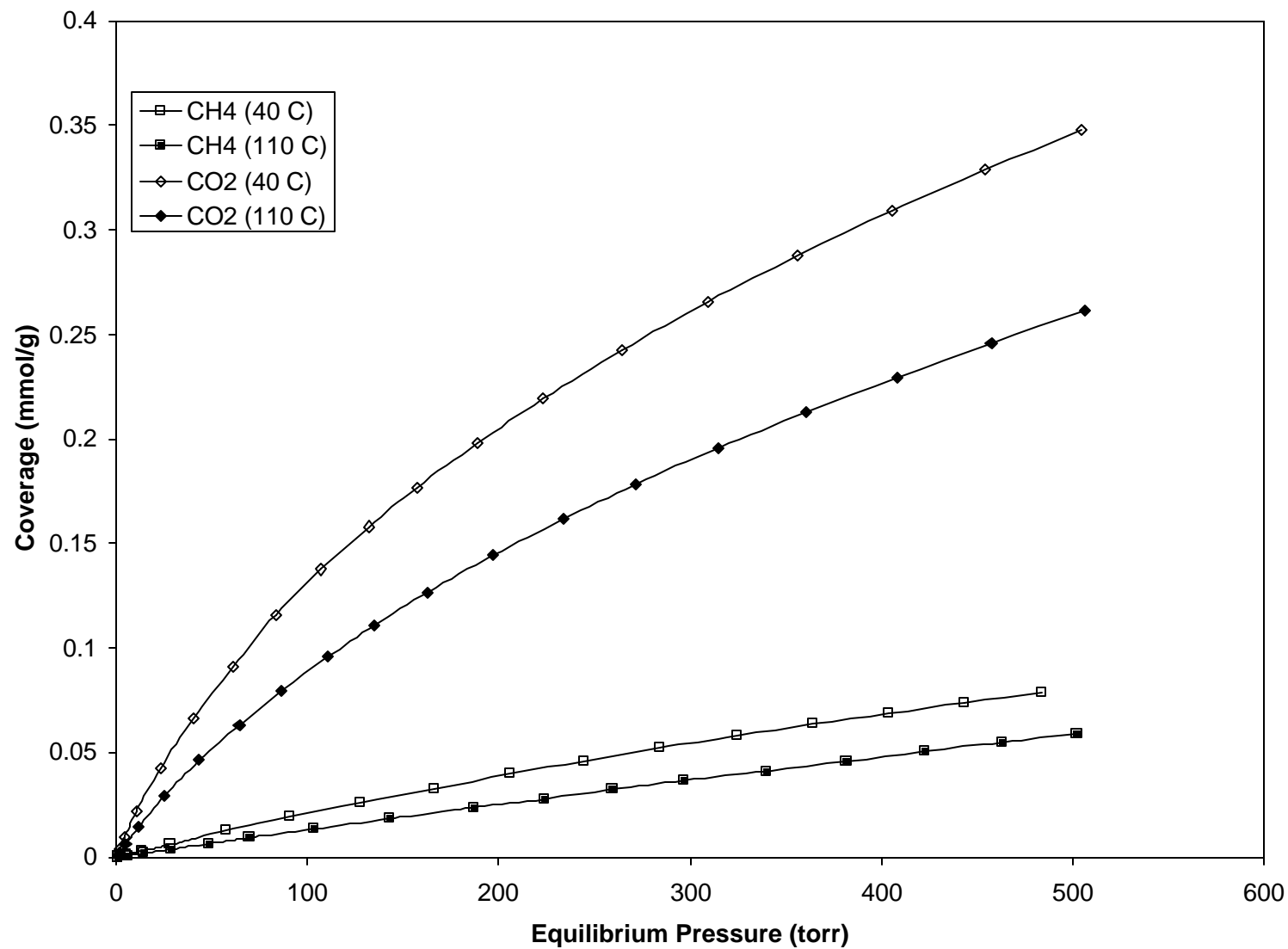
Figure 8. Adsorption on Illinois #6 Coal

Figure 9. Heats of Adsorption on Illinois #6 Coal